2007

2007 Sedimentary Geology Molas.pdf

James E. Evans

Available online at www.sciencedirect.com
ScienceDirect
Sedimentary Geology 195 (2007) 161 – 181
Sedimentary Geology
www.elsevier.com/locate/sedgeo

Integrated loessite-paleokarst depositional system, early Pennsylvanian Molas Formation, Paradox Basin, southwestern Colorado, U.S.A.

James E. Evans *, Jason M. Reed [1]

Department of Geology, Bowling Green State University, Bowling Green, Ohio 43403, USA

Received 13 January 2006; received in revised form 14 July 2006; accepted 19 July 2006

Abstract

Mississippian paleokarst served as a dust trap for the oldest known Paleozoic loessite in North America. The early Pennsylvanian Molas Formation consists of *loessite facies* (sorted, angular, coarse-grained quartz siltstone), *infiltration facies* (loess redeposited as cave sediments within paleokarst features of the underlying Mississippian Leadville Limestone), *colluvium facies* (loess infiltrated into colluvium surrounding paleokarst towers) and *fluvial facies* (siltstone-rich, fluvial channel and floodplain deposits with paleosols). The depositional system evolved from an initial phase of infiltration and colluvium facies that were spatially and temporally related to the paleokarst surface, to loessite facies that mantled the paleotopography, and to fluvial facies that were intercalated with marine-deltaic rocks of the overlying Pennsylvanian Hermosa Formation. This sequence is interpreted as a response to the modification of the dust-trapping ability of the paleokarst surface. Loess was initially eroded from the surface, transported and redeposited in the subsurface by the karst paleohydrologic system, maintaining the dust-trapping ability of the paleotopographic surface. Later, the paleotopographic surface was buried when loess accumulation rates exceeded the transport capacity of the karst paleohydrologic system. These changes could have occurred because of (1) increased dust input rates in western Pangaea, (2) rising base levels and/or (3) porosity loss due to deposition within paleokarst passageways.

Keywords: Loessite; Paleokarst; Terra rossa; Paleohydrology; Paleoclimatology

1. Introduction

Significant accumulations of silt-sized eolian sediment (dust or loess) require a source area, transport mechanism (prevailing winds of sufficient energy) and depositional mechanism (Tsoar and Pye, 1987). Traditionally, glaciated areas have been considered the major source of loess (Pye, 1987), but recent studies have shown that modern deserts provide significant dust loadings to surrounding areas (e.g., Nettleton and Chadwick, 1996). In modern deserts, production of significant amounts of loess is dependent on seasonal runoff, the concentration of weathering detritus (including silt) in dry washes or wadis, and then remobilization by wind (Yaalon and Ganor, 1973). The most effective dust transport mechanisms are high latitude frontal systems or low latitude monsoonal-influenced circulation systems (Soreghan, 1992).

* Corresponding author. Tel.: +1 419 372 2414; fax: +1 419 372 7205.
E-mail addresses: evansje@bgsu.edu (J.E. Evans), Jason.Reed@epa.state.oh.us (J.M. Reed).
[1] Present address: Ohio Environmental Protection Agency, 3232 Alum Creek Drive, Columbus, OH 43207, USA. Tel.: +1 614 728 3873.

0037-0738/$ - see front matter © 2006 Elsevier B.V. All rights reserved.
doi:10.1016/j.sedgeo.2006.07.010

Because particles >20 μm are transported within the lowest few 10 s of meters of the atmospheric boundary layer, dust trapping is enhanced by topography, such as deposition in the lee of topographic features (Tsoar and Pye, 1987). Other effective dust traps are moisture and vegetation (Cegla, 1969), and infiltration into porous sediments (Pye, 1987), talus (Goossens, 1995) or rock fractures (Villa et al., 1995). After deposition, eolian silt may be remobilized by wind or surface water erosion, and also because of the high permeability of silt, subsurface erosion by groundwater piping or sapping can be a major mechanism of sediment redistribution (Bal and Buursink, 1976).

In western North America, late Mississippian (Visean or Meramecian) sea level fall (Ross and Ross, 1985; Veevers and Powell, 1987) exposed an extensive carbonate shelf sequence to a range of humid tropical to subtropical weathering conditions. Over the ensuing 34 m.y., a broad paleokarst plain developed, with >50 m paleorelief and an extensive network of subsurface paleocaves, sinkholes and fissures (DeVoto, 1980; Sando, 1988; Palmer and Palmer, 1995).

This paper focuses on how this late Mississippian paleokarst surface served as a dust trap for early Pennsylvanian loess. The presence of loess in the cave sediments and overlying the paleokarst surface documents significant paleoclimatic change between more humid conditions of the late Mississippian, and the increasing aridity and seasonality of the late Pennsylvanian–Permian megamonsoonal paleoclimate of western Pangaea. In addition, this study highlights the complex relationship between the dust-trapping ability of the paleokarst surface and the accumulation of the eolian sediments. To be specific, the maintenance of the dust-trapping system was dependent upon the ability of the karst paleohydrological system to erode, transport and redeposit the eolian sediment. Once the accumulation rates of loess exceeded the transport capacity of the paleohydrologic system, the depositional system infilled paleocave passages, buried the karst paleotopography, and transitioned upwards to a fluvial and marine-deltaic depositional system.

2. Background

2.1. Late Mississippian paleokarst

The Mississippian Leadville Limestone is found in the Paradox Basin, San Juan Basin, San Juan Mountains, Maroon Trough and Central Colorado Mineral Belt (Armstrong et al., 1992). In the study area in southwestern Colorado (Fig. 1), paleokarst features in the Leadville Limestone include tower karst (kegelkarst) with approximately 25 m relief (Maslyn, 1977), solution valleys (poljes) with 100–200 m relief (DeVoto, 1988), paleo-sinkholes (dolines), sediment-filled joints and fractures (grikes) and breccias (DeVoto, 1988; Hall, 1990). This paper also reports phreatic tubes, "breakout domes" (e.g., Loucks, 1999), surficial erosion surfaces (rillenkarren), probable solution pans (kamenitzas) and mosaic and crackle breccias (Fig. 2). Previous studies reported that speleothems are rare in the Central Colorado Mineral Belt (DeVoto, 1988; Tschauder et al., 1990). In contrast, our work has found that flowstone sheets, dripstones, stalagmites and cave pearls can be locally common in the study area. The history of paleokarst in the Leadville Limestone is complicated by an earlier episode of intraformational surficial karst several meters thick, overprinted by later events (DeVoto, 1988; Hall, 1990), several episodes of pre- and post-karst dolomitization (Beaty, 1985; Horton and DeVoto, 1990; Hall, 1990), late Paleozoic and Laramide (Cretaceous–Paleogene) hydrothermal alteration (Hall, 1990; Landis and Tschauder, 1990; Symons et al., 2000), and modern karst (Teller and Welder, 1983).

2.2. Red siliciclastic sediment

There are red siliciclastic sediments (previously described as shale, claystone or silty claystone) both within the Leadville Limestone and overlying it. The overlying unit was labeled the Molas Formation (Cross et al., 1904) and was interpreted as a terra rossa (residual) paleosol that was reworked upwards (Merrill and Winar, 1958). The Molas Formation is considered early Pennsylvanian (Bashkirian–Moscovian or Morrowan–early Desmoinesian) in age and varies from 0 to 30 m thick throughout the study area (Merrill and Winar, 1958; Armstrong et al., 1992). Revisions of the age and stratigraphy of the Molas Formation are given in Fig. 3 and discussed later in this paper.

Problems with the terra rossa interpretation were evident even to those who proposed it. There is <1% insoluble residue in the Leadville Limestone, requiring dissolution of >1500 m of carbonate to account for the thickness of terra rossa (Merrill and Winar, 1958). Compositional mismatches between the insoluble residue and red siliciclastic sediment were noted but explained as diagenetic (Merrill and Winar, 1958). The terra rossa explanation does not agree with observations that the Molas Formation can also be found overlying non-carbonate rocks (Baars, 1966). Merrill and Winar (1958) noted that significant accumulation of insoluble residue in pore spaces would have reduced flow rates necessary to form karst features. These and other related problems with the terra rossa explanation have been discussed elsewhere (Evans, 2002).

Based upon the dominance of quartz silt with hematitic kaolinite grain-coatings, we propose that the

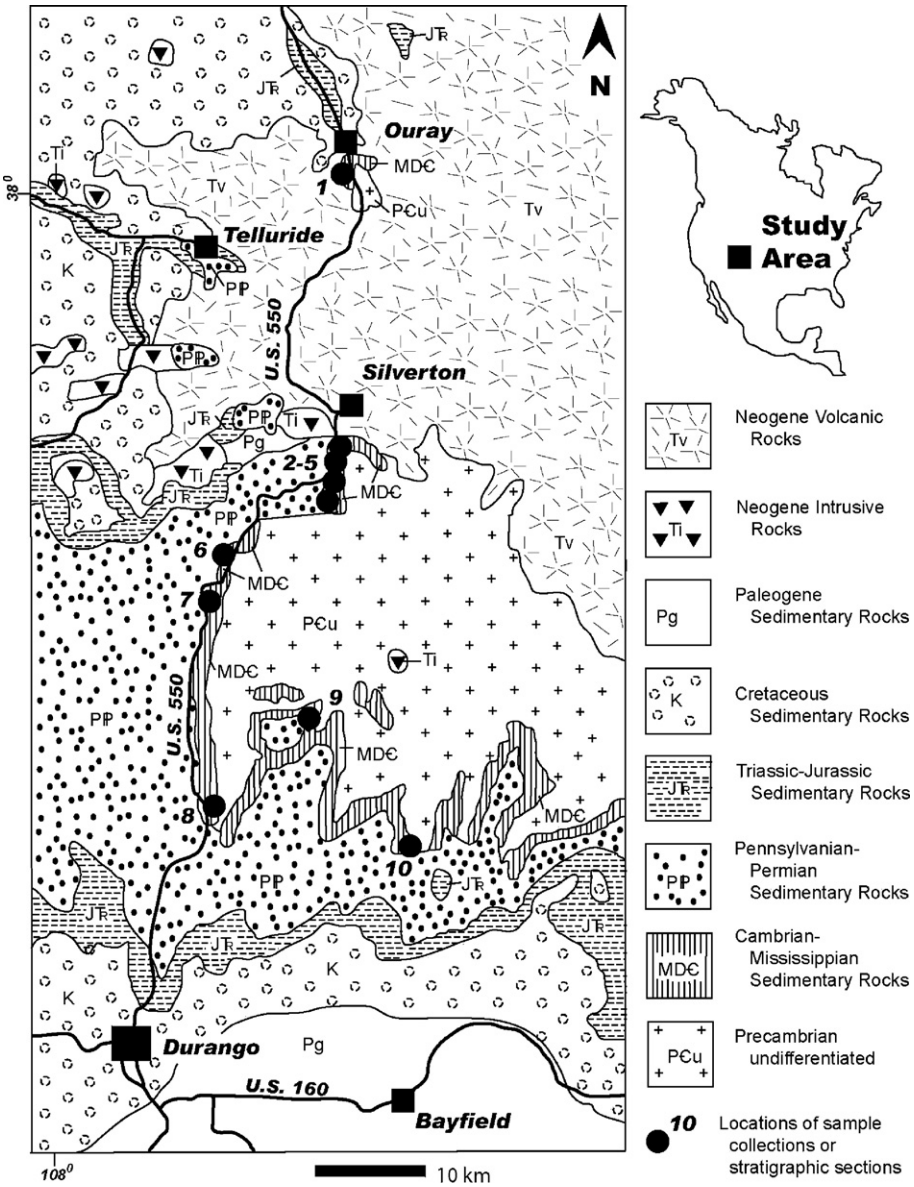

Fig. 1. Map of the study area in southwestern Colorado, U.S.A., showing the outcrop belt of the Leadville Limestone (vertical stripes) and overlying Pennsylvanian rocks (large stipples). Study sites are: (1) Ouray, (2) Sultan Creek, (3) Molas Lake (north), (4) Molas Lake (south), (5) Molas Creek, (6) Coal Bank Pass, (7) Purgatory, (8) Rockwood Quarry, (9) Stag Mesa and (10) Vallecito Creek.

Molas Formation was a loessite that buried and partially infiltrated into underlying paleokarst of the Mississippian Leadville Limestone. This explanation is more in accord with recent understandings that late Cenozoic terra rossa soils are accretionary deposits with significant inputs of eolian dust (Pye, 1987). For modern terra rossa soils, this evidence includes compositional and textural mismatches between the soil and limestone parent material (Macleod, 1980; Danin et al., 1983), geochemical provenance links to dust sources (Syers et al., 1969; Rapp, 1984; Muhs et al., 1990), problems related to requiring unreasonable carbonate dissolution rates (Bricker and MacKenzie, 1971; Macleod, 1980), occurrence of terra rossa soils over buried lichens and karst exposure surfaces, and remote sensing data demonstrating dust transport (Yaalon and Ganor, 1973, 1979).

3. Methods

Measured stratigraphic sections are shown in Fig. 4. Colors are described using the Munsell Color Chart (Goddard et al., 1948). Petrographic samples were

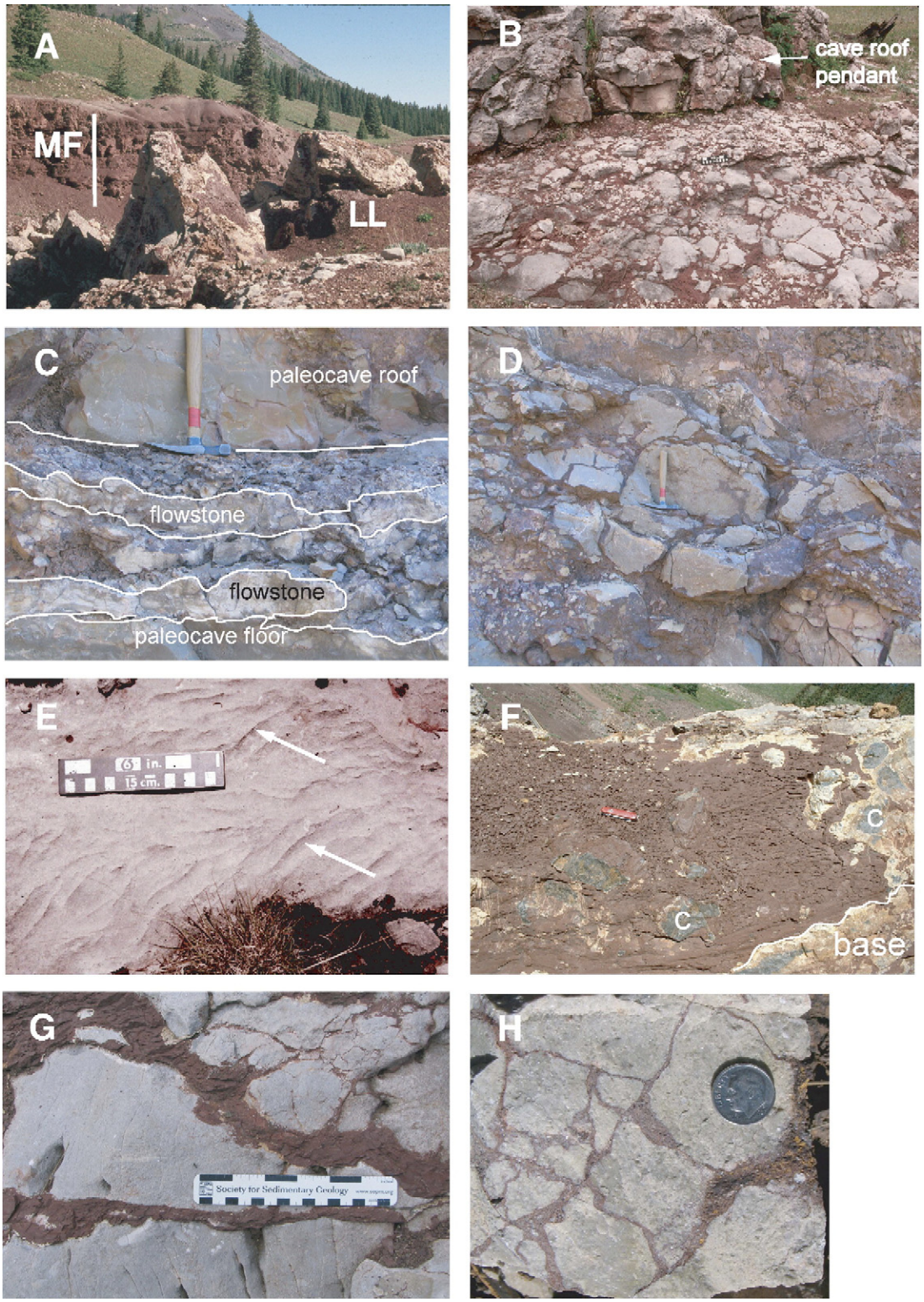
A
MF
LL
B
cave roof
pendant
C
paleocave roof
flowstone
flowstone
paleocave floor
D
E
6 in.
15 cm.
F
C
C
base
G
Society for Sedimentary Geology
H

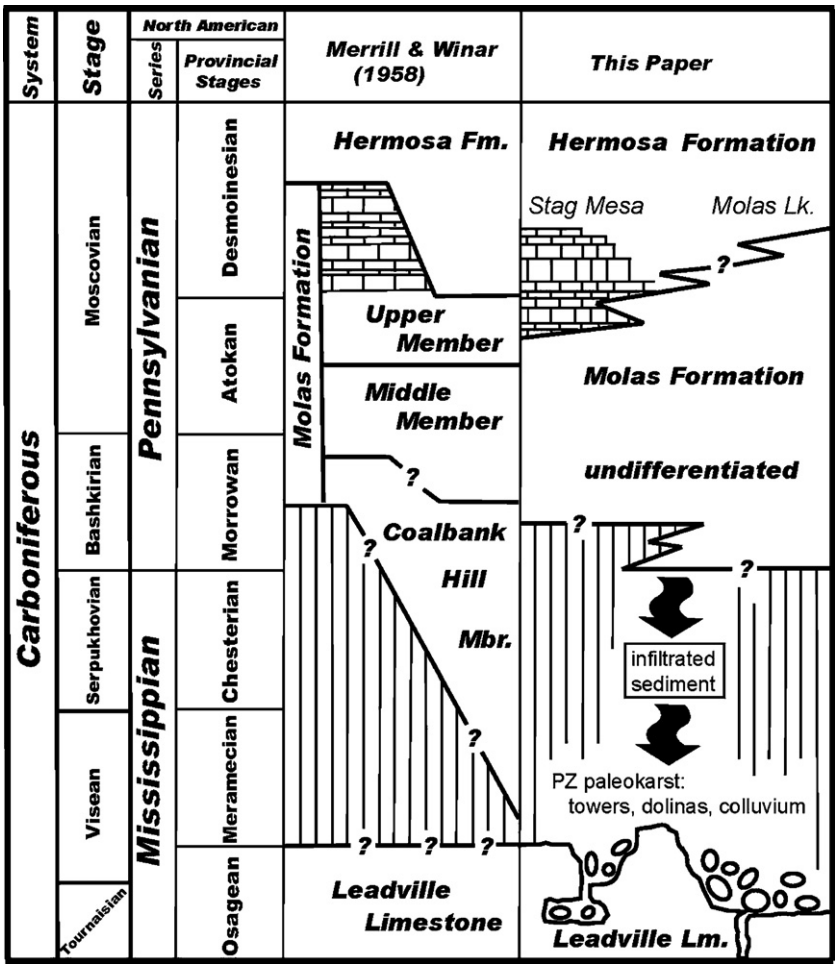

Fig. 3. Stratigraphic revision of the Molas Formation proposed by this study. The three stratigraphic subdivisions (Coalbank Hill, Middle, and Upper Members) would be eliminated, portions of the upper unit reassigned to the Hermosa Formation, and the upper and lower boundaries redefined. See text for discussion.

prepared using standard techniques. Grain size point counts were conducted at 100× magnification, using an eyepiece micrometer and counting stage with $n>400$ counts per slide. Thin-section point count data was converted to equivalent sieve data using the methods of Harrel and Eriksson (1979). Grain size statistics were from Folk and Ward (1957). Scanning electron microscope (SEM) analyses were performed on a Hitachi 2700 scanning electron microscope with a LaB_6 filament to obtain high magnification samples of prepared images, using the analytical methods of Krinsley and Doornkamp (1973) and Welton (1984). Energy dispersive X-ray spectrometry (EDS) was conducted using an EDX-4 spectrometer and evaluated using the methods of Welton (1984) and Postek et al. (1980). X-ray diffraction (XRD) analyses used a Phillips APD 3520 X-ray spectrometer

Fig. 2. Photographs of paleokarst features in the Leadville Limestone. (A) Paleokarst tower in the Leadville Limestone (LL) in the foreground and outcrop of the overlying Molas Formation (MF) in the background. Vertical line shows the location of the 14 m Molas Lake (north) section. (B) Portion of a breakout dome, showing the intact cave roof pendant over the chaotic breccias and infiltrated red siliciclastic sediment (scale = 15 cm). (C) Portion of a phreatic tube showing the smooth paleocave walls and multiple infill of flowstone sheets, debrites and fluvial cave sediments (hammer = 28 cm). (D) Portion of a paleo-sinkhole (doline) including fragmented portions of mosaic breccias with a mixture of chaotic breccias and red siliciclastic sediment (hammer = 28 cm). (E) Exposed surface of the Leadville Limestone–Molas Formation contact showing rillenkarren which is overlain elsewhere by loessite (scale = 15 cm). (F) Possible solution pan (kamenitza) showing a bowl-like structure, with etched side walls, chert clasts (C) with white weathering rinds, and red siliciclastic sediments (knife = 9 cm). (G) Example of chaotic and mosaic breccias, consisting of solution etched limestone clasts and red siliciclastic sediment (scale = 15 cm). (H) Example of crackle breccias (coin = 1.8 cm).

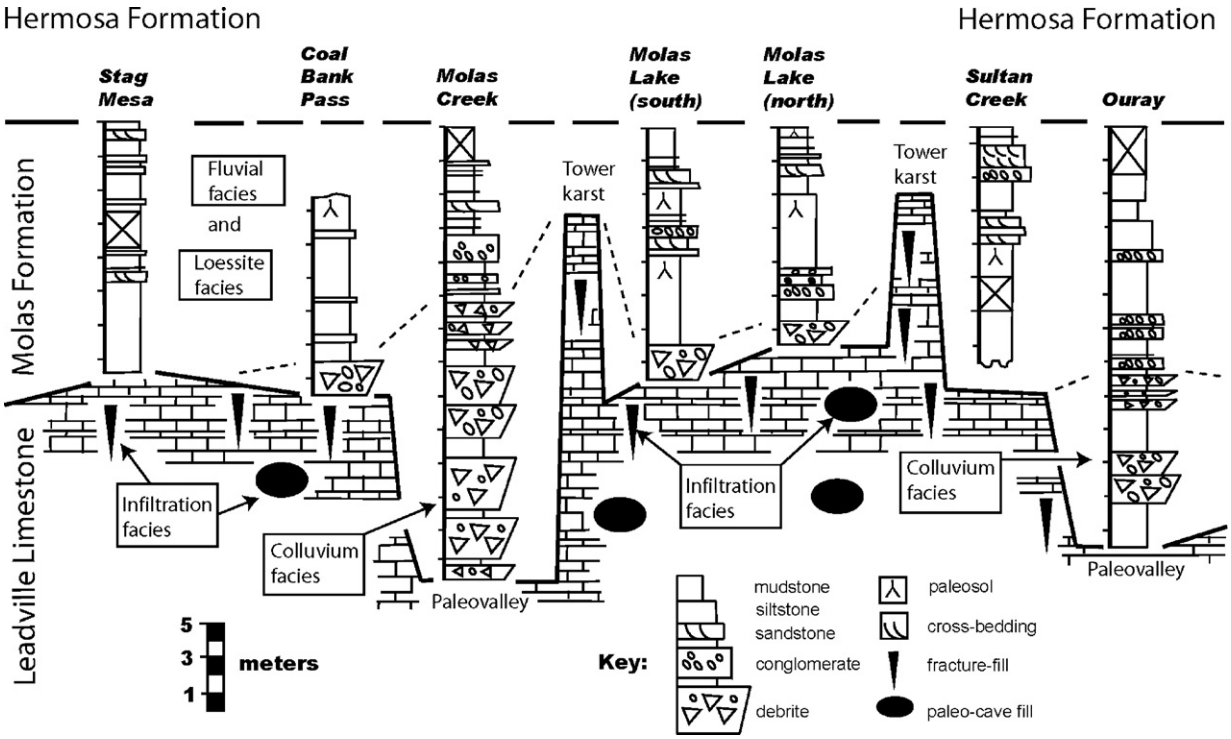

Fig. 4. Correlation diagram of the larger stratigraphic sections measured for this study (locations given in Fig. 1). The intercalated upper contact with the Hermosa Formation is used for line of reference. Note three inferred paleokarst towers and intervening solution valleys.

with Cu K-alpha radiation, and the diffractograms were interpreted using the methods of Moore and Reynolds (1989).

4. Results

4.1. Revised age and stratigraphy

Merrill and Winar (1958) subdivided the Molas Formation into the ascending Coalbank Hill Member, Middle Member and Upper Member (Fig. 3). The Coalbank Hill Member was interpreted as a terra rossa paleosol containing solution-rounded boulders of Leadville Limestone (Wengerd and Strickland, 1954; Merrill and Winar, 1958; Szabo and Wengerd, 1975). The Middle Member was interpreted as reworked terra rossa and related terrigenous deposits, and the Upper Member was interpreted as marine on the basis of illite-bearing shales and fossiliferous limestones in the upper part of the unit at a single locality, Stag Mesa (Merrill and Winar, 1958).

There have been many problems with the stratigraphic subdivisions proposed by Merrill and Winar (1958). First, it was difficult to recognize the base of the Molas Formation ("transition zone" of Cross et al., 1905). Merrill and Winar (1958) defined the Leadville Limestone–Molas Formation contact based upon the lateral continuity of limestone beds. This definition raises serious problems in the field, because outcrops are random exposures of a contact that is a paleokarst surface with up to 100–200 m paleorelief. Second, in the absence of limestone (found only at one locality), Merrill and Winar (1958) could not differentiate the Middle and Upper Members in the field. We find this is true because these strata consist of loessite with varying proportions of fluvial channels and reworked loessite (Fig. 4). Third, previous studies have found the limestone of Stag Mesa has identical fossil content to limestones in the overlying Hermosa Formation (e.g., Larsen and Cross, 1956; Wengerd and Matheny, 1958; Baars and Ellingson, 1984; Reed, 2000). We observe that the absence of siliciclastic silt within the limestone of Stag Mesa makes it lithologically different from the rest of the Molas Formation, but similar to the limestones of the Hermosa Formation. Finally, detailed sections indicate that the Molas Formation–Hermosa Formation contact is intercalated (i.e., a type of vertical transition zone where Molas Formation red siltstones are interbedded with Hermosa Formation limestones, illite-bearing marine shales and feldspathic sandstones). Accordingly, we believe that the limestone of Stag Mesa and related strata should be reassigned to the Hermosa Formation (Fig. 3).

Thus, we agree with Murray (1958), who argued that limestones attributed to the upper part of the Molas Formation in the Maroon Trough are better considered part of the overlying unit (Hermosa Formation).

In summary, we propose that the stratigraphic subdivisions of the Molas Formation be abandoned, and the unit be considered undifferentiated (Fig. 3). We find that the "Coalbank Hill Member" represents infiltration of Molas Formation into paleokarst passages of the Leadville Limestone (see Discussion). The confusion about defining the base of the Molas Formation (or recognizing the presence or absence of the "Coalbank Hill Member") is simply an artifact of the arbitrary exposure of paleokarst features at any particular outcrop. The "Middle" and "Upper" Members are indistinguishable in the field because they both consist of loessite with varying proportions of interbedded fluvial deposits (Fig. 4). Because of the intercalated contact between the Molas Formation and Hermosa Formation, and because of the fossil content of the limestone of Stag Mesa, we believe the limestones and marine shales of the "Upper Member" should be reassigned to the latter unit. These recommendations are in accord with subsurface studies of the Paradox Basin, where the Molas Formation cannot be subdivided (e.g., Clair, 1958).

This is not a minor stratigraphic disagreement. A number of studies have attributed the presence or absence of "members" of the Molas Formation as evidence for Pennsylvanian tectonic uplift or subsidence of great regional significance throughout this part of North America (e.g., Merrill and Winar, 1958; Spoelhof, 1976; Weimer, 1980; Baars et al., 1987). As we have shown, the arbitrary definition of these "units" means that their presence or absence at any particular outcrop does not have any tectonic significance (Evans, 2002).

4.2. Composition

4.2.1. Molas Formation

The Molas Formation consists of primarily of quartz, with lesser amounts of kaolinite, hematite and goethite (Fig. 5A). SEM and XRD analyses show that the accessory minerals are in the form of hematitic kaolinite grain-coatings or argillans (Figs. 5 and 6). EDS analysis shows the presence of ferric iron in the argillans, which is responsible for giving the unit a typical moderate red (5R 5/4 to 5R 4/6) color. The identical process is responsible for the reddening of late Cenozoic loess (Pye, 1987). Throughout the Molas Formation, there are spots or patchy zones along fractures where the unit is greenish gray (5GY 6/1) in color. EDS analysis shows that these are reduction spots where hematite has been lost. The reduction spots may be related to Cenozoic hydrothermal activity associated with precious metal mineralization of the Silverton Caldera.

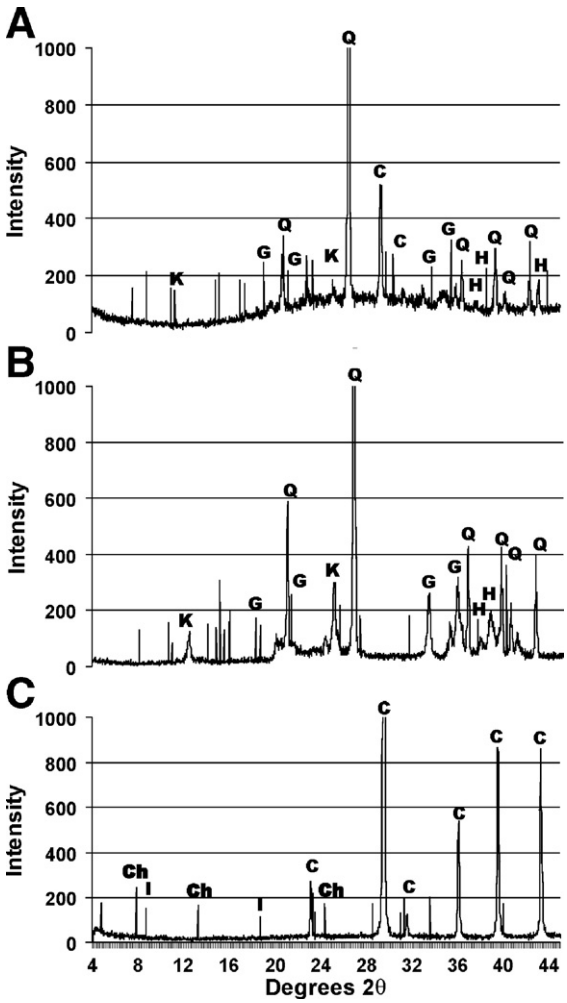

Fig. 5. Composition of the Molas Formation and Leadville Limestone determined by X-ray diffraction. (A) Red loessite of the Molas Formation consists of quartz with hematite and kaolinite grain coatings. (B) Red siltstone from paleocave deposits in the underlying Leadville Limestone showing identical composition to the overlying loessite. (C) Unaltered portion of the Leadville Limestone showing calcite with an insoluble residue of illite and chlorite. Abbreviations used: C=calcite, Ch=chlorite, G=goethite, H=hematite, I=illite, K=kaolinite, Q=quartz.

4.2.2. Leadville Limestone cave sediments

The red siliciclastic sediments within the paleokarst features of the late Mississippian Leadville Limestone (Fig. 5B) are compositionally identical to the overlying early Pennsylvanian Molas Formation (Fig. 5A) but differ considerably from the insoluble residue of the Leadville Limestone (Fig. 5C). The insoluble residue of the Leadville Limestone consists of clay-sized illite and chlorite

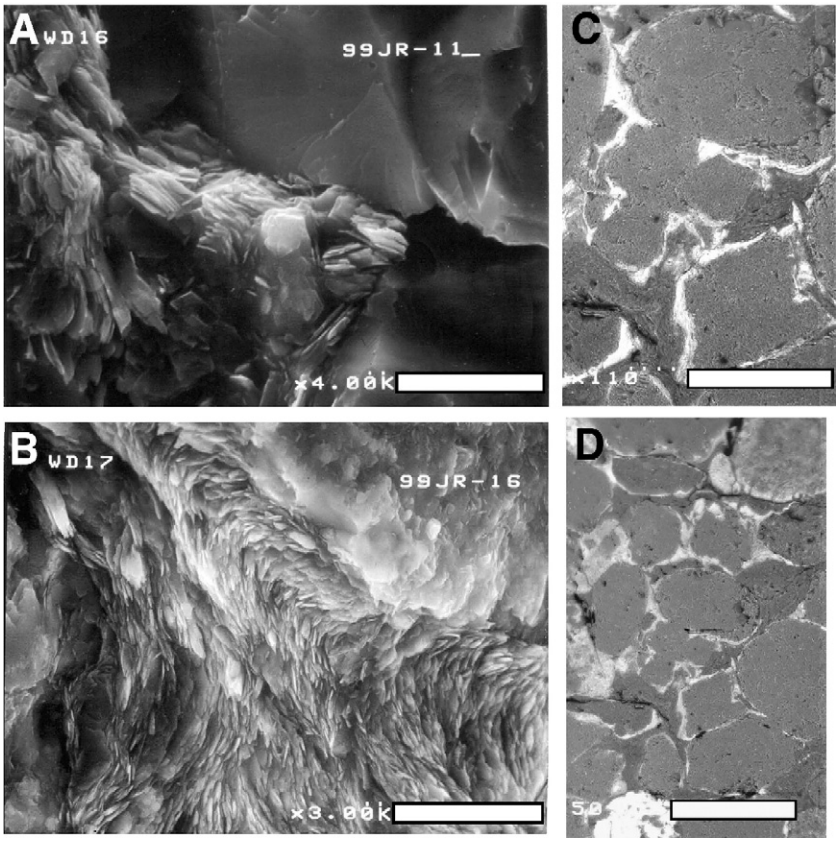

Fig. 6. Scanning electron microscope images of the Molas Formation. (A) Secondary electron SEM image showing the platy nature of the clay grain-coatings (magnification 400,000×, scale bar = 7.5 μm). (B) Secondary electron SEM image showing the platy nature of the clay grain-coatings (magnification 300,000×, scale bar = 10 μm). (C) Backscattered electron image of quartz silt grains (light gray areas), showing clay grain-coatings (white areas) and secondary goethite accumulations (dark areas). Magnification 110,000× (scale bar = 60 μm). (D) Similar backscatter image to (C), showing pore-filling carbonate cement (dark gray). Magnification 50,000× (scale bar = 50 μm).

(Merrill and Winar, 1958, this study). In contrast, the siliciclastic paleocave sediments are silt-sized quartz with hematitic kaolinite argillans, as discussed above.

4.3. Texture

Most of the Molas Formation consists of moderately sorted, coarse-grained silt with symmetrical skewness (Fig. 7A and Table 1). The paleocave sediments in the underlying Leadville Limestone are texturally identical to the loessite (shown as infiltration facies in Fig. 7B and Table 1). Other parts of the Molas Formation are very poorly sorted deposits that have strongly positive skewness or excess fines (Table 1). The presence of the excess fines in the silt sizes is interpreted as loess infiltration into surficial paleokarst colluvium (Fig. 7C) and as fluvial deposits with a high percentage of reworked loess (Fig. 7D). The former deposits are bimodal (with histogram peaks for coarse silt and clay) while the latter deposits are polymodal (medium-grained sand, coarse silt and clay).

The paleocave sediments are clearly redeposited loess. A detailed evaluation of a continuous section through the upper part of the Leadville Limestone shows that the inherited loessite textural signature can be traced downward >12 m at one locality (Fig. 8). At other locations, paleocave sediments that are entirely siltstone were recovered >30 m below the Molas Formation–Leadville Limestone contact.

4.4. Lithofacies

The Molas Formation consists of four facies assemblages: loessite facies, infiltration facies, colluvium facies and fluvial facies (Table 2). The relative importance of each facies assemblage varies geographically. In general, the infiltration facies and colluvium facies are found at the lower contact with the Leadville Limestone, while the

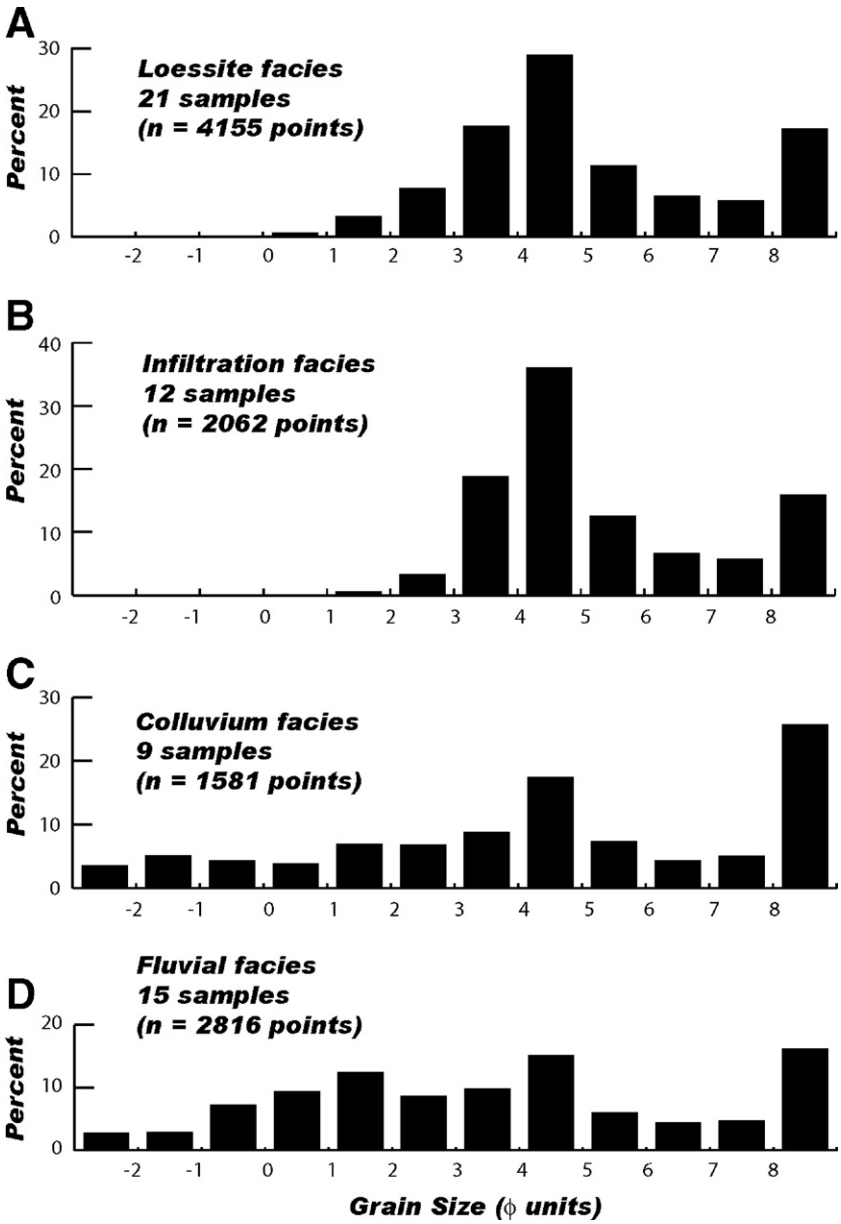

Fig. 7. Composite grain size histograms from thin-section point counts ($n > 400$ points per sample). (A, B) The loessite and infiltration (paleocave sediment) histograms show moderately sorted, bimodal distributions with peaks in the coarse silt (4–5 ϕ) and clay (> 8 ϕ) ranges. (C) The colluvium facies (infiltrated matrix into debrites or talus deposits) shows a similar, but very poorly sorted distribution. (D) The fluvial facies is also very poorly sorted, with coarse silt (4–5 ϕ) and clay (> 8 ϕ) peaks, but also sand (−1 ϕ to 4 ϕ). Both of the latter show a strong positive skewness or an excess of fine-grained sediment (Table 1).

importance of loessite facies and fluvial facies increase stratigraphically upwards through the unit (Fig. 4).

4.4.1. Loessite facies

The loessite facies assemblage primarily consists of massive, homogeneous, red, coarse-grained hematitic quartz siltstone to very fine-grained sandstone (lithofacies SSm). Bedding is poorly developed over intervals up to 6 m thick (Fig. 9A). Polished sections can reveal a faint lamination (Fig. 9B) related to subtle grain size changes. Thin sections reveal angular–subangular, quartz silt with occasional "outsized" clasts of subangular–subrounded quartz sand (Fig. 9C and D). Discontinuities in bedding include thin (< 1 cm) mudstone drapes, rare mudcracked or brecciated surfaces, poorly developed paleosols and interbedded colluvium facies or fluvial facies. The

Table 1
Summary grain size statistics[a] for the Molas Formation

Property	Loessite facies	Infiltration facies	Colluvium facies	Fluvial facies
Mode	4.5 ϕ	4.5 ϕ	4.5 ϕ	4.5 ϕ
Median	4.6 ϕ	4.9 ϕ	5.6 ϕ	4.4 ϕ
Mean	4.0 ϕ	4.3 ϕ	2.2 ϕ	2.3 ϕ
Standard deviation	1.0 ϕ	0.9 ϕ	3.0 ϕ	2.6 ϕ
Skewness	0.0	0.0	0.5	1.6
Sorting class	Moderately sorted	Moderately sorted	Very poorly sorted	Very poorly sorted
Skewness class	Symmetrical	Symmetrical	Strongly positive skewness	Strongly positive skewness

[a] Grain size statistics from Folk and Ward (1957).

interbedded pond deposits seen in younger Paleozoic loessites in the region (Johnson, 1989) were not observed in the Molas Formation.

Paleosol features include faint blocky ped structures, minor pedogenic slickensides, vertical root structures (including rhizoliths and drab-halo rootcasts), gradational boundaries and greenish-gray mottling (Fig. 9E). Paleosols superimposed on loessites are classified as lithofacies SSp. The rhizoliths are vertical tubes, between 2 mm and 4 cm in diameter, that bifurcate downwards to depths of < 95 cm, and are either filled by sand or pore-filling calcite spar (Fig. 9F). Hematitic kaolinite grain-coatings (argillans) are pervasive except in mottles. The mottling is difficult to evaluate because in places the blebs and spots appear associated with rootcasts and other paleosol features (e.g., Chan, 1999), but in other places the association is not so clear (Fig. 9G) and the features could be interpreted as later reduction-spot phenomenon. Molas Formation paleosols are very similar to the late Pennsylvanian–Permian loessite paleosols in western North America described by others (Johnson, 1989; Chan, 1999; Tramp et al., 2000; Kessler et al., 2001). Because

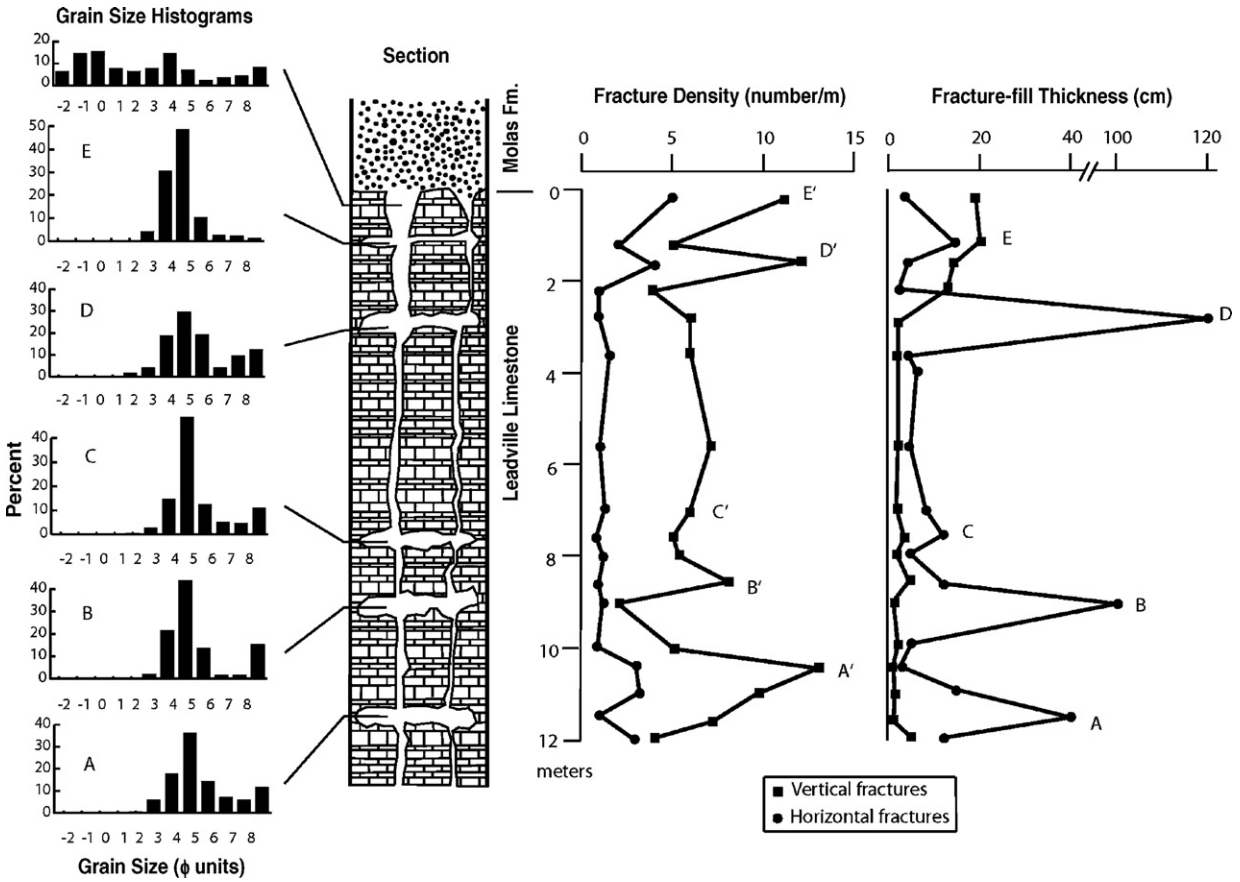

Fig. 8. Vertical section of the upper 12 m of the Leadville Limestone in Rockwood Quarry. Paleocaves are indicated as A–E. The thickness of each (filled) paleocave is given on the right. Samples collected from each paleocave were evaluated for grain size (histograms on the left). The results show an inherited loess signature (4–5 ϕ size class) down into the paleokarst. Also note how vertical fractures show solution-widening near the top (right column) and how vertical fracture density increases locally (A′–E′) directly above the paleocaves (middle column).

Table 2
Lithofacies in the Molas Formation

Facies association	Lithofacies	Texture	Structures	Interpretation
Loessite	SSm	Siltstone	Massive	Loessite
	SSp	Siltstone	Pedogenic features	Paleosol (in loessite)
Infiltration (allochthonous cave deposits)	Dmm	Diamict	Massive	Debrite (cave sediment)
	Dms	Diamict	Crudely stratified	Debrite (cave sediment)
	Gm	Conglomerate	Massive	Cave fluvial channel-fill
	Fl	Siltstone–mudstone	Laminated	Cave flood deposit
	Fm	Mudstone	Massive	Cave flood waning-flow deposit
	Jl	Fissure-fill deposits	Laminated	Multiple infill of grikes
	Jm	Fissure-fill deposits	Massive	Infill of grikes
Colluvium	Br	Breccia	Massive	Rock-fall talus
	Dmm	Diamict	Massive	Debrite
	Dms	Diamict	Crudely stratified	Debrite
	SSm	Siltstone	Massive	Loessite (interbedded)
Fluvial	Gm	Conglomerate	Massive	Fluvial channel-fill
	St	Sandstone	Trough x-beds	Fluvial 3-D dunes
	Sr	Sandstone	Ripple lamination	Fluvial ripples
	Se	Sandstone, intraclasts	Massive	Channel bank failures
	SSm	Siltstone	Massive	Loessite (interbedded)
	SSp	Siltstone	Pedogenic features	Paleosol (in loessite)
	Fl	Siltstone–mudstone	Laminated	Flood deposit
	Fm	Mudstone	Massive	Overbank deposit
	Fp	Mudstone	Pedogenic features	Paleosol (in mudstone)

of rudimentary development, the paleosols are classified as calcic protosols (Mack et al., 1993), and probably indicate rapid burial of these surfaces by accumulating loess. Similar, modern loess soils have been described from semiarid regions with seasonal rainfall, such as Afghanistan. Those modern loess soils are calcixerollic xerochrepts with weak, subangular blocky peds in ochric epipedons <25 cm thick, that overlie cambic horizons containing soil cutans and pedotubules (Bal and Buursink, 1976). The high porosity and low bulk density of these silty soils promotes subsurface piping, subsidence and soil collapse features especially when wetted (Bal and Buursink, 1976).

4.4.2. Infiltration facies

The infiltration facies assemblage represents allochthonous siliciclastic sediment introduced to paleo-sinkholes (dolines), paleocaves, phreatic passages and fractures or joints (grikes) in the underlying Leadville Limestone. The allochthonous sediments include debrites (lithofacies Dmm and Dms), fluvial cave sediments (lithofacies Gm, Sr, SSm, Fl and Fm) and fissure-fill sediments (lithofacies Jl and Jm). Fig. 10A shows a polished section through a paleocave mudflow, which included limestone, chert and red siltstone clasts. The fluvial cave sediments (Fig. 10B) include clast-supported conglomerates containing limestone and nodular chert clasts, eroded speleothem clasts and red siltstone intraclasts. These are overlain by silty sandstone showing lamination or climbing-ripple lamination, laminated or massive siltstone and siltstone–claystone rhythmites (Fig. 10C), which often are capped with a mudcracked clay drape on the upper bedding surfaces (Fig. 10D). The fluvial cave sediments typically overlie scours or vadose channels. The bimodal gravel and silt–clay texture is probably an artifact of the source from cave-collapse limestone and chert clasts admixed with redeposited loess. The presence of debrites, fluvial conglomerates, scours and upper flow regime sedimentary structures suggest high-energy flow events through these paleocave passages, while rapid dewatering is suggested by the mudcracks. These deposits are interpreted as ephemeral, high-energy flood-flows through phreatic passageways, and the resulting deposits can be considered inundites.

The fissure-fill sediments can be massive or laminated. These consist of mixtures of redeposited loess and parautochthonous karst breccias. Horizontal bedding in these deposits is interpreted as multiple episodes of in-wash of surficial materials and/or episodes of spalling of materials from the walls of the fractures or joints. Lamination that is primarily vertical (parallel to the walls of the fissure) is interpreted to represent multiple episodes of re-opening of filled fissures due to shifting of the underlying blocks in breakout domes (Fig. 10E).

These allochthonous deposits are interbedded with parautochthonous cave sediments (such as chaotic, mosaic and crackle breccias) and with autochthonous cave sediments (such as flowstones, dripstones, stalagmites

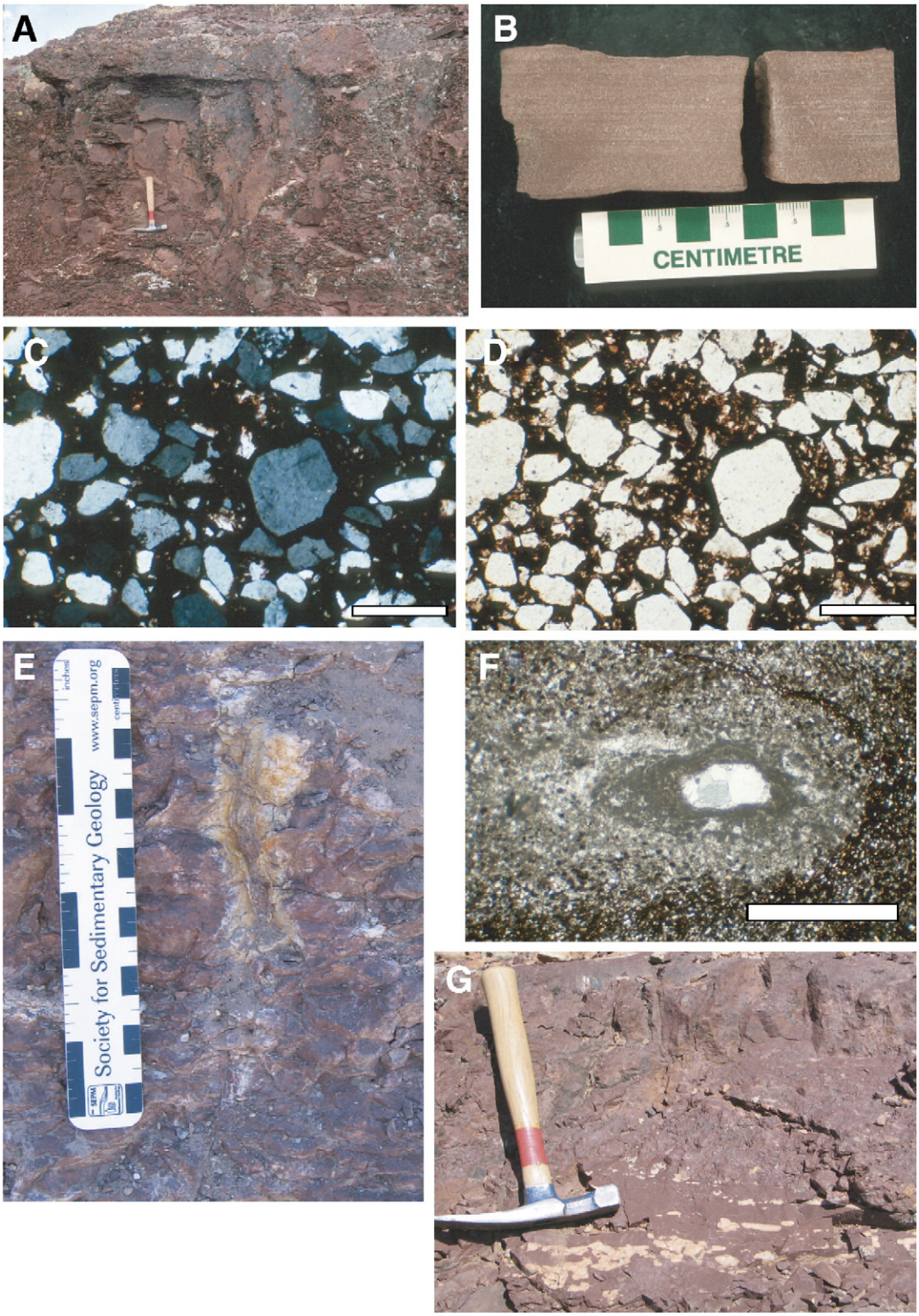
A
B
CENTIMETRE
C
D
E
Society for Sedimentary Geology
www.sepm.org
F
G

and cave pearls). The breccias consist of fossiliferous limestone and chert set in a matrix of red siltstone and smaller carbonate fragments. The breccia fabric ranges from widely displaced clasts in chaotic breccias (Fig. 2G) to slightly displaced clasts in crackle breccias (Fig. 2H). Although the clasts are highly angular, there are numerous examples of solution rounding and embayment. Many chert clasts are fossiliferous and are surrounded by weathering rinds. The flowstones occur as massive or laminated sheets of calcite that are interbedded with breccias and fluvial cave sediments. Flowstone sheets drape some surfaces or individual clasts (Fig. 10F). There are examples of fragments of eroded flowstone sheets incorporated as clasts in fluvial cave sediments. Dripstones have been observed on bedding surfaces as small mound-like accumulations, including stalagmites (Fig. 10G). Cave pearls are sand-sized (50–100 μm diameter) and consist of a nucleus and cortex that consists of concentrically banded isopachous calcite spar (Fig. 10H).

4.4.3. Colluvium facies

The colluvium facies assemblage consists of rock-fall talus and debrites surrounding paleokarst towers (Maslyn, 1977). Colluvium deposits are interbedded with meter-scale loessite beds (lithofacies SSm) infilling the solution valleys between adjacent paleokarst towers (Fig. 4). The debrites (lithofacies Dmm and Dms) are typically massive, matrix-supported diamicts consisting mostly of angular chert clasts (Fig. 11A). They show non-erosive bases and abrupt upper contacts, and are typically interbedded with loessite (Fig. 11B). Clasts in the debrites consist of nodular chert that is clearly derived from the Leadville Limestone because many contain silicified Mississippian marine fossils, and some are internally banded. The rock-fall talus deposits are disorganized, clast-supported breccias (lithofacies Br) that consist of very poorly sorted, angular or solution-rounded limestone clasts and subangular–subrounded nodular chert clasts, ranging from sand- to boulder-size, with an infiltrated red siltstone matrix (Fig. 11C). In some cases, impact fabrics (sagging of the underlying sediment layers beneath a clast) suggest that individual talus clasts fell directly into soft loess at the base of the karst towers (Fig. 11D). Lithologically, rock-fall talus deposits in the colluvium facies are very similar to chaotic karst-collapse breccias described earlier. Important differences are: the generally smaller grain-size, lack of association with mosaic or crackle breccias, lack of association with interbedded speleothems, the stratigraphic position above the paleokarst surface and lateral proximity to karst towers.

4.4.4. Fluvial facies

The fluvial facies assemblage consists of clast-supported pebble conglomerates (lithofacies Gm), sandstone with red siltstone intraclasts (lithofacies Se), rare cross-bedded sandstones (lithofacies St) and ripple-laminated sandstone (lithofacies Sr), interbedded with thick sequences of siltstone (lithofacies SSm) and mudstone (lithofacies Fl and Fm). The single-story lenticular channels had average dimensions of approximately 2 m deep by 40 m wide (Fig. 12A). The margins of the channels were gently sloping, with no evidence of cutbanks or bank stability, in accord with the silty composition of the bank materials (Fig. 12B). Typically, the channel deposits are well rounded, moderately sorted, chert pebble conglomerate with occasional red siltstone intraclasts (Fig. 12C). The chert clasts commonly have red hematitic kaolinite grain-coatings, similar to the siltstones. True shales (mudstones and silty mudstones, as opposed to siltstones) have a darker color red (dusky red or 5R 3/4) that is visible in the field (Fig. 12A) and form meter-scale beds interbedded with siltstone. Paleosols are weakly developed calcic protosols similar to those described from the loessite facies (lithofacies SSp and Fp). The relatively few, shallow and weakly developed fluvial channels suggest a system of silt-dominated, ephemeral channels interbedded with floodplains dominated by accumulating loess.

4.4.5. Depositional environment

In summary, the Molas Formation was principally a loessite depositional system, consisting of loessite facies and related, loess-influenced fluvial and colluvial environments. Molas Formation loessite shows identical features to other described loessites in the geological record, such as a dominantly sorted, angular, coarse-grained silt texture, quartz composition, ferruginous cement, clay grain-coatings, red color, general absence of stratification, mantling of paleotopography and poorly developed calcareous paleosols (Edwards, 1979; Johnson, 1989; Chan, 1999; Kessler et al., 2001). The most unusual characteristic of the

Fig. 9. Photographs of the loessite facies of the Molas Formation. (A) Typical outcrop view of massive to crudely bedded siltstone (hammer = 28 cm). (B) Polished section showing faint lamination in loessite (scale = 7 cm). (C) Photomicrograph showing typical angular quartz siltstone with occasional sand-sized clast, crossed-polars (scale bar = 50 μm). (D) Same image with plane-polar light (scale bar = 50 μm). (E) Photograph of bifurcating drab-halo rootcasts in a calcic protosol (scale = 15 cm). (F) Photomicrograph of a cross-section through a rhizolith in a fluvial mudstone (scale bar = 100 μm). (G) Photograph of mottling in the loessite. In this case, mottling appears stratigraphically controlled and related spatially to paleosols. However, in other cases, mottling appears to be reduction spots that are randomly placed or localized along vertical joints (hammer = 28 cm).

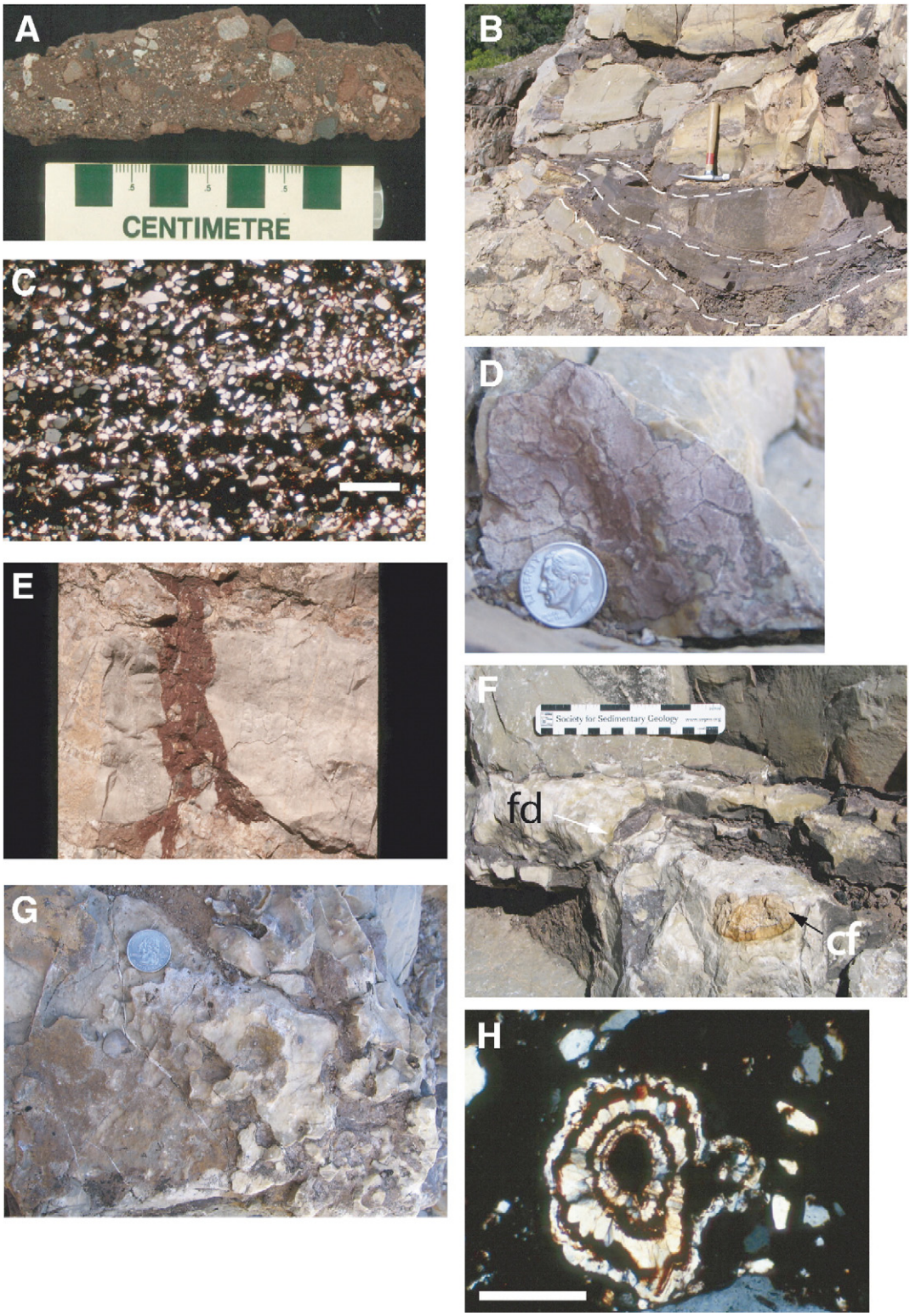
A
CENTIMETRE
B
C
D
E
F
Society for Sedimentary Geology
fd
cf
G
H

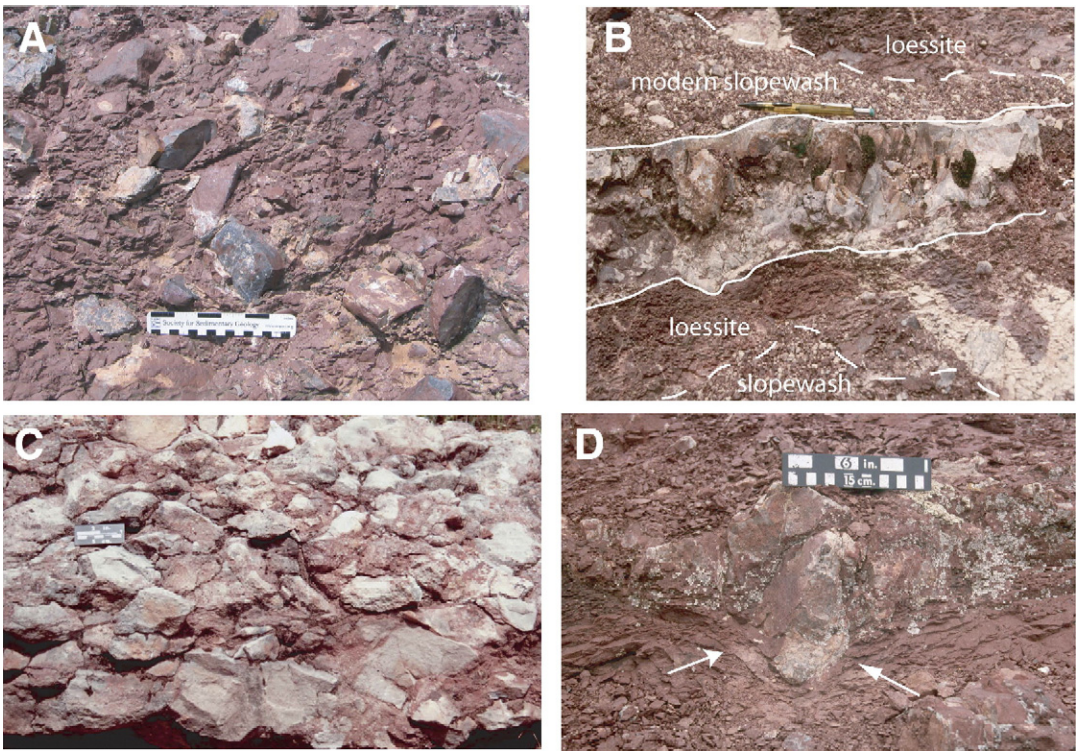

Fig. 11. Photographs of the colluvium facies of the Molas Formation. (A) Photograph of a debrite (lithofacies Dmm), a massive, matrix-supported chert cobble diamict with red siltstone matrix (scale = 15 cm). (B) Photograph of a thin (<20 cm thick) debrite interbedded with loessite, showing planar, non-erosive base with abrupt upper contact, which is partially obscured by modern slope wash (pencil = 15 cm). (C) Photograph of talus, showing a clast-supported, disorganized, chert cobble breccia with a red siltstone matrix (scale = 5 cm). (D) Example of an impact structure that probably formed when an individual talus block fell into the loess accumulating near the base of the paleokarst tower (scale = 15 cm).

Molas Formation was its interaction with a paleokarst depositional surface. These interactions included redeposition of loess into open paleokarst passageways and interbedding of loess with surficial karst colluvium.

5. Discussion

5.1. Origin of the cave sediments

The red siliciclastic sediments within paleokarst features of the Leadville Limestone are compositionally (Fig. 5) and texturally (Fig. 7) identical to the overlying loessite of the Molas Formation, and these paleocave sediments retain their inherited loessite textural signature >12 m below the Molas Formation–Leadville Limestone contact (Fig. 8). Further, the allochthonous paleocave sediments can be interpreted as debrites, fluvial cave sediments and fissure-fill sediments (Fig. 10). The allochthonous cave sediments are interbedded with parautochthonous cave sediments (rubble, chaotic and mosaic breccias) and autochthonous cave sediments (flowstone, dripstone, stalagmites and cave pearls). Accordingly, we interpret these paleocave deposits as the result of surface and subsurface erosion and transport

Fig. 10. Photographs of the infiltration facies of the Molas Formation. (A) Polished section of a mudflow deposit recovered from a paleocave in the Leadville Limestone (scale = 7 cm). (B) View of a phreatic tube infilled by a succession of three inundites. Each inundite consists of a thin basal pebble or intraclasts layer overlain by laminated silty sandstone and laminated siltstone, often with mudcracked clay drapes at the top. (C) Photomicrograph of a laminated cave sediment, interpreted as siltstone–claystone rhythmites from the Leadville Limestone (scale bar = 200 μm). (D) Mudcracked upper bedding surface of a fluvial cave deposit in the Leadville Limestone (coin=1.8 cm). (E) Photograph of a laminated fissure-fill deposit (scale bar = 15 cm). (F) Photograph of interbedded flowstones and red siliciclastic cave sediments, showing multiple episodes of paleocave infill, flowstone drape (fd) and cross-section of a cave formation (cf) such as a stalagmite (scale = 15 cm). (G) Bedding plane exposure of the base of a paleocave, showing complex microtopography. The microtopography consists of small dripstone impact craters (some later infilled by red cave sediment) surrounded by elevated dripstone rims which consists of laminated calcite (coin = 2.5 cm). (H) Photomicrograph showing a cross-section of a cave pearl (concentrically banded, isopachous calcite spar) in red siliciclastic cave sediment (scale bar = 50 μm).

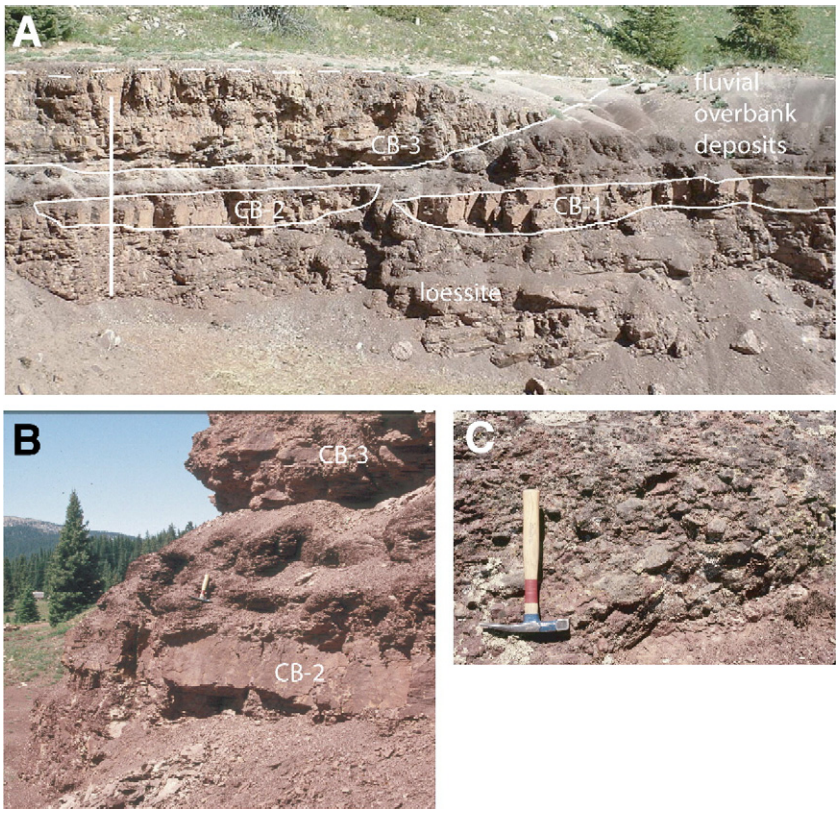

Fig. 12. Photographs of the fluvial facies of the Molas Formation. (A) View of three channel bodies (CB) interbedded with loessite (base) or fluvial overbank mudstones (top). Note color contrast between loessite and fluvial mudstones (vertical scale bar = 5 m). (B) View of loessite (base), thin fluvial channel (CB-2) and overlying fluvial mudstone (hammer = 28 cm). (C) Imbrication in fluvial pebble conglomerates (hammer = 28 cm).

of loess, and subsequent redeposition within open paleokarst passages.

The structure of the paleokarst in the Leadville Limestone suggests a repeated sequence of events: (1) formation of phreatic tubes by solution-widening of joints, (2) partial to complete in-filling of phreatic tubes by allochthonous sediments, (3) tube enlargement by roof stoping and (4) phreatic tube collapse as vadose zone karst features with a complex history of infilling by cave-collapse breccias, allochthonous sediment infill and multiple episodes of calcite and silica cementation. The resulting features have been termed "breakout domes" by Loucks (1999) and represent sequential fall in regional paleo-groundwater surfaces. The superposition of tiered breakout domes implies repeated episodes of falling of the piezometric surface that was probably controlled by downcutting of solution valleys. We interpret studies of the Leadville Limestone from the Central Colorado Mineral Belt (Tschauder et al., 1990) and of the coeval Redwall Limestone of Arizona (Troutman, 2004) to show similar sequences of interbedded fluvial cave sediments and speleothems beneath cave collapse breccias.

5.2. Timing and paleoclimate of paleokarst formation

The Leadville Limestone and its stratigraphic equivalents were part of a widespread Mississippian carbonate shelf sequence that covered much of western North America (DeVoto, 1988; Armstrong et al., 1992; Fouret, 1996). The non-karsted portions of the Leadville Limestone and its equivalents typically have <1% insoluble residue contents, consisting of clay-sized illite, chlorite or smectite (Merrill and Winar, 1958; McKee and Gutschink, 1969; Meyers, 1988; Reed, 2000). Exceptions include minor amounts of eolian (rounded and frosted) quartz sand in the lower part of the Leadville Limestone in the Central Colorado Mineral Belt (Banks, 1970), and "very small" (silt-sized?) quartz in the coeval Redwall Limestone of Arizona (McKee and Gutschink, 1969) of possible eolian origin. In summary, it is possible that small amounts of eolian sediments were deposited in this extensive carbonate platform during the Mississippian.

Subaerial exposure of the carbonate shelf starting in the late Mississippian has been linked both to glacio-eustatic sea level fall (Ross and Ross, 1985; Veevers and

Powell, 1987) and to regional uplift ("Ancestral Rocky Mountains") related to the Ouachita Orogeny (Armstrong et al., 1992). Karstification of late Mississippian carbonates was extensive throughout western North America, producing >50 m paleorelief and extensive networks of karst passageways during an exposure interval of approximately 34 m.y. (Sando, 1988; DeVoto, 1988; Palmer and Palmer, 1995). The timing of the karstification is constrained by multiple lines of evidence. First, karst formation did not lead to collapse features in overlying units such as the Molas Formation (cf. Pelechaty et al., 1991). Second, magnetopolarity data indicates the Leadville Limestone was subjected to post-karst dolomitization at about 308±6 Ma (Symons et al., 2000). Third, the early Pennsylvanian Molas Formation overlies surficial paleokarst features such as rillenkarren, and varies in thickness across solution valleys and dolines (this study). Finally, the paleocave sediments themselves were derived from the Molas Formation, and were interstratified with multiple layers of flowstone and cave-collapse breccias. In summary, the evidence suggests that Leadville Limestone karst formation began in the late Mississippian (Visean or Meramecian), and overlapped at least in part with the deposition of the Molas Formation (Bashkirian–Moscovian or Morrowan–early Desmoinesian).

It is recognized that karst can form in a wide range of climates (Wright, 1988). Paleokarst features in the Leadville Limestone suggest humid-region weathering and possibly fluctuations between wetter–drier phases of climate. The major evidence for humid-region weathering is tower karst (kegelkarst) near Molas Lake (Maslyn, 1977) and in central Colorado (Hall, 1990). The towers near Molas Lake are each >100 m in diameter and have >25 m paleorelief (Maslyn, 1977). Examples of modern kegelkarst are found exclusively in humid-tropical regions such as southeast China, Vietnam, New Guinea and Jamaica (White, 1990). Other evidence that is suggestive, but not conclusive, of humid-region weathering includes the scale of solution valleys (100–200 m deep), the extensive network of solution-widened joints (cutters), large numbers of dolines and their size (maximum dimensions of 450 m in diameter and 75 m deep), and regional thinning of the unit (DeVoto, 1988). Evidence for fluctuating wet–dry climate is suggested by the presence of tiered breakout domes discussed above, multiple levels of paleocaves (DeVoto, 1988) and the stratigraphy of individual paleo-sinkhole deposits suggesting multiple episodes of ponding and draining (DeVoto, 1988). Recognition of breakout domes (Loucks, 1999) is particularly significant, because they are created when former phreatic passageways enter the vadose zone due to falling regional water tables. When the former phreatic passages are dewatered, they become enlarged by multiple episodes of cave-roof collapse, and modified by dissolutional excavation and infilling by breccias, speleothems and allochthonous sediments. Meanwhile, new phreatic passages formed beneath the previous ones. Production of multiple levels of breakout domes thus suggests progressively falling piezometric surfaces (Loucks, 1999). The infilling of these tiered breakout domes by sediment derived from the Molas Formation shows that the loess was deposited on a paleokarst surface that was deepening due to regional base level fall. It is probable this was controlled, at least locally, by the downcutting of solution valleys.

5.3. Loessite provenance and paleoclimate

The Molas Formation is the oldest known Paleozoic loessite in North America. Previous workers have emphasized the importance of increasing amounts of eolian dust in western North America during the Pennsylvanian and Permian. Soreghan (1992) attributed the increasing eolian dust component of marine rocks during the late Pennsylvanian–early Permian to the northward drift of Pangaea from tropical to subtropical latitudes and the onset of monsoonal circulation systems related to final assemblage of the supercontinent. In addition to the presence of loessite, other evidence for late Pennsylvanian–early Permian aridification includes the presence of subaerial debrites, playa lakes, ephemeral stream deposits and carbonate paleosols (Dinterman et al., 2000; Kessler et al., 2001). Evidence for wet–dry climatic cycles includes the abundance of hematite (Kessler et al., 2001), presence of vertic paleosols (Dinterman et al., 2000; Tramp et al., 2000), alternating loessite-paleosols sequences (Miller and McCahon, 2000) and alternating loessite-marine carbonates with surficial microkarst (Cecil et al., 2000).

Because the loessites in the Molas Formation did not produce paleocurrent indicators, and because they are almost entirely composed of quartz, the source of the Molas Formation silt is still unknown. There is better evidence from the younger eolian deposits in this region. Soreghan et al. (2002) have used detrital zircon ages to show that late Pennsylvanian–early Permian loessites were derived from weathering of uplifted Precambrian basement rocks. In addition, the determination of specific basement rock source areas showed that later Pennsylvanian paleowinds had both northerly and southerly directions (consistent with fluctuations of the inter-tropical convergence zone), while early Permian paleowinds were westerly (consistent with the onset of monsoonal circulation). Paleocurrent data from Permian–Jurassic

cross-bedded eolian sandstones confirm the significance of prevailing westerlies and monsoonal circulation in this portion of North America (Loope et al., 2004).

The deposition of the Molas Formation loessite on the paleokarst surface of the Leadville Limestone preceded these conditions, and provides a benchmark for the significant paleoclimatic changes in this region from humid tropical production of tower karst to the increasing aridification and monsoonal circulation of the late Paleozoic. As a "tropical" loessite, the Molas Formation matches descriptions of late Cenozoic loess from tropical regions in South America, such as intense clay illuviation and dominance of grain-coatings consisting of kaolinite, hematite and goethite (Iriondo and Krohling, 1997). Although Dinterman et al. (2000) remark on the unexpected dominance of eolian deposits and other arid region features near the paleo-equator, modern studies document significant dust transport over distances of >7000 km (Muhs et al., 1990; Beget et al., 1993).

5.4. Evolution of the trap mechanism

Dust-trapping mechanisms can include topography (Tsoar and Pye, 1987), moisture and vegetation (Cegla, 1969), and infiltration into porous sediments (Pye, 1987), talus (Goossens, 1995) or rock fractures (Villa et al., 1995). Paleokarst has not been previously identified as a dust-trapping mechanism, although it obviously unifies several of the previous mechanisms. Although rhizoliths can be observed in the Molas Formation, the weak paleosol development probably indicates vegetative trapping was minor compared to topographic and infiltration mechanisms.

Only a few studies of modern caves have suggested that cave sediments act as an archive for eolian dust or loess. Musgrave and Webb (2004) interpreted the "red earth" cave sediments of southeastern Australia as redeposited eolian dust derived from the central Australian Desert. Tremul (2002) showed provenance links between cave sediments and modern dust in Italy. DeLumley (1965) suggested that increased eolian activity during Pleistocene cold periods explained patterns of cave sedimentation in southern France. In this study, paleokarst apparently acted as a dust trap for the oldest known Paleozoic loessite in North America.

The intense karstification of the Leadville Limestone beginning in the late Mississippian produced paleorelief that typically ranges from 30 to 50 m (maximum of 100–200 m reported by DeVoto, 1988), and probably served as an effective initial dust-trap. However, it is likely that the Molas Formation would have rapidly buried this surface, without some additional trapping mechanism. Late Cenozoic desert dust accumulation rates range from 10 to 16 cm/k.y. in the Middle East (Nettleton and Chadwick, 1996), implying that burial of most of the Leadville paleotopography was possible within 188–500 k.y.

Paleokarst adds a dimension to the trapping mechanism because of the evidence for subsurface sediment redistribution. The Leadville Limestone contains abundant allochthonous sediment in the form of debrites, fluvial cave sediments and fissure-fill sediment. In addition, these allochthonous sediments are texturally and compositionally identical to the overlying Molas Formation loessite. Finally, the absence of fluvial deposits in the lower part of the Molas Formation suggests that infiltration and subsurface run-off were important during the deposition of the loessite.

Studies of modern loess and loessial soils have documented extensive groundwater piping processes (Jones, 1990). These deposits are characterized by low cohesion, easily transported grain sizes and typically low organic matter content. Previous studies document seepage piping network growth rates of >150 m/year and subsequent soil collapse or gully formation (Galarowski, 1976). A hummocky topography with sinkhole-like structures is produced, with overall subsidence rates up to 1.8 m/year (Bal and Buursink, 1976). Evidently, modern seepage piping and subsidence rates can be at least one order of magnitude above typical desert loess accumulation rates (e.g., Nettleton and Chadwick, 1996). This suggests that a paleokarst surface has the potential of being a long-term dust trap, because the paleorelief could be maintained as long as some of the loess was redistributed by erosion, transport and redeposition in the subsurface.

Bosch and White (2004) have shown that there is a dynamic relationship between flow through a karst aquifer and sediment transport. Higher flow rates have greater competence and capacity through phreatic passageways; however, sediment deposition can clog passageways and reduce porosity and permeability. In other words, the sediment capacity of these subsurface flow systems is affected by transient conditions.

The presence of tiered breakout domes (and their siliciclastic sediment infill) in the Leadville Limestone document falling regional piezometric surfaces during the time of deposition of the Molas Formation. The Leadville Limestone paleokarst system was expanding vertically by downward growth during this phase. Such growth created accommodation space for redistribution of the loess. Changes in the paleohydrologic system are indicated in the upper part of the Molas Formation: the loess mantled the paleotopography and the depositional system transitioned upward to a loessite-fluvial depositional system,

and eventually to the fluvial-deltaic depositional system of the overlying Hermosa Formation.

Three factors could have driven this change. First, increases in loess depositional rates could have overwhelmed the capacity of the paleohydrological system to redistribute the sediment. Evidence in support of this would include the studies documenting increasing evidence of aridity throughout the late Paleozoic in this region (Soreghan, 1992). Second, rising base levels would terminate the growth of the karst system. Evidence in support of this includes the presence of fluvial channel and overbank deposits in the upper part of the Molas Formation and marine transgression of the Hermosa Formation. Finally, deposition of redistributed loess within the karst passageways of the Leadville Limestone may have reduced the capacity of the paleohydrological system. It is difficult to evaluate this possibility except to note the presence of significant debrites, fluvial cave sediments and fissure-fill sediments document that some infilling of karst passageways certainly did occur.

6. Summary and conclusions

The Molas Formation represents a complex loessite depositional system, consisting of loess deposits and related paleokarst, colluvium and fluvial environments. Loess that was initially trapped on the underlying paleokarst surface was subjected to surface and subsurface erosion, transport and redeposition within paleokarst passageways (phreatic caves, breakout domes, dolines and grikes) of the Leadville Limestone. The infiltration of surficial loess into karst colluvium surrounding paleokarst towers constituted the colluvium facies. Subsequently, the loessite facies and colluvium facies were interbedded until the paleokarst landscape was completely mantled by loess. The overlying loess is interbedded with thin fluvial deposits with a significant component of reworked loess. The upper part of the Molas Formation (loessite facies and fluvial facies) is an intercalated contact with the overlying marine-deltaic Hermosa Formation.

Tiered breakout domes in the Leadville Limestone document falling piezometric surfaces and indicate that the downward growth of the karst system over time created accommodation space for the redistribution of loess. This redistribution prevented, for a time, the burial of the paleokarst surface by accumulating loess, maintaining the topographic dust-trapping mechanism. Eventually, loess buried the paleokarst surface, transitioning upwards to a loessite-fluvial depositional system and then a fluvial-deltaic depositional system. These changes could have been due to: (1) increased dust accumulation rates in the region, (2) rising base levels or (3) the effect of deposition of the allochthonous siliciclastic sediment (redistributed loess) in the karst passageways on the capacity of the subsurface transport system.

Acknowledgements

We wish to thank C.F. Kahle and C.M. Onasch for their advice about the regional geology, and J. Farver for assistance with SEM analyses. The manuscript was significantly improved by suggestions from David B. Loope and an anonymous reviewer.

References

Armstrong, A.K., Mamet, B.L., Repetski, J.E., 1992. Stratigraphy of the Mississippian System, south-central Colorado and north-central New Mexico. USGS Bull. 1787-EE, 1–22.

Baars, D.L., 1966. Pre-Pennsylvanian paleotectonics—key to basin evolution and petroleum occurrences in the Paradox Basin. Am. Assoc. Pet. Geol. Bull. 50, 2082–2111.

Baars, D.L., Ellingson, J.A., 1984. Geology of the western San Juan Mountains. In: Brew, D.C. (Ed.), Geological Society of America, Rocky Mountain Section. Field Trip Guidebook, vol. 37, pp. 1–45.

Baars, D.L., Ellingson, J.A., Spoelhof, R.W., 1987. Grenadier fault block, Coalbank to Molas Passes, southwest Colorado. Rocky Mountain Section Centennial Field Guide. Geological Society of America, Boulder, Colorado, pp. 343–348.

Bal, L., Buursink, J., 1976. An inceptisol formed in calcareous loess on the "Dast-i-Esan Top" plain in Afghanistan: fabric, mineral, and trace element analysis. Neth. J. Agric. Sci. 24, 17–42.

Banks, N.G., 1970. Nature and origin of early and late cherts in the Leadville Limestone, Colorado. Geol. Soc. Amer. Bull. 81, 3033–3048.

Beaty, D.W., 1985. The oxygen and carbon isotope geochemistry of the Leadville Formation. In: DeVoto, R.H. (Ed.), Sedimentology, Dolomitization, Karstification, and Mineralization of the Leadville Limestone (Mississippian), Central Colorado. SEPM Mid-year Meeting Guidebook, vol. 6, pp. 71–78.

Beget, J.E., Keskinen, M., Severin, K., 1993. Mineral particles from Asia found in volcanic loess on the island of Hawaii. Sediment. Geol. 84, 189–197.

Bosch, R.F., White, W.B., 2004. Lithofacies and transport of clastic sediment in karstic aquifers. In: Sasowsky, I.D., Mylroie, J. (Eds.), Studies of Cave Sediments. Kluwer Academic-Plenum Press, New York, pp. 1–22.

Bricker, O.P., MacKenzie, F.T., 1971. Limestones and red soils of Bermuda: discussion. Geol. Soc. Amer. Bull. 81, 2523–2524.

Cecil, C.B., Dulong, F.T., West, R.R., 2000. Climatic controls on middle Pennsylvanian sedimentation in the continental United States. Geol. Soc. Am. Abstr. Programs 32 (7), A-254.

Cegla, J., 1969. Influence of capillary ground moisture on eolian accumulation of loess. Pol. Acad. Sci., Bull., Geol.-Geogr. Ser. 17 (1), 25–27.

Chan, M.A., 1999. Triassic loessite of north-central Utah: stratigraphy, petrophysical character, and paleoclimate implications. J. Sediment. Res. 69, 477–485.

Clair, J.R., 1958. Subsurface stratigraphy of the Pennsylvanian of the Paradox Basin. Symposium on the Pennsylvanian Rocks of Colorado

and Adjacent Areas. Rocky Mountain Association of Geologists, Denver, pp. 31–46.

Cross, C.W., Howe, E., Ransome, F.L., 1904. Silverton, Colorado. USGS Geologic Atlas, Folio 120, 34 pp.

Cross, C.W., Spencer, A.C., Irving, J.D., Emmons, W.H., 1905. Needle Mountains, Colorado. USGS Geologic Atlas, Folio 131, 138 pp.

Danin, A., Gerson, R., Carty, J., 1983. Weathering patterns on hard limestone and dolomite by endolithic lichens and cyanobacteria: supporting evidence for eolian contribution to terra rossa soil. Soil Sci. 136, 213–217.

DeLumley, H., 1965. Evolution des climates quaternaries d'apres le remplissage des grottes de Provence et du Langhedoc mediterraneen. Bull. de l'Assoc. Fran. pour l'etude du Quaternaire, vol. 2, pp. 165–170.

DeVoto, R.H., 1980. Mississippian stratigraphy and history of Colorado. In: Kent, H.C., Porter, K.W. (Eds.), Colorado Geology. Rocky Mountain Association of Geologists, Denver, pp. 57–70.

DeVoto, R.H., 1988. Late Mississippian paleokarst and related mineral deposits, Leadville Formation, central Colorado. In: James, N.P., Choquette, P.W. (Eds.), Paleokarst. Springer-Verlag, New York, pp. 278–305.

Dinterman, P.A., Mack, G.H., Leeder, M., Oerez-Arlucea, M., 2000. Paleoclimatic control on early Permian fluvial to eolian transition in New Mexico. Geol. Soc. Am. Abstr. Programs 32 (7), A254.

Edwards, M.B., 1979. Late Precambrian glacial loessites from Norway and Svalbard. J. Sediment. Petrol. 49, 85–91.

Evans, J.E., 2002. Reinterpretation of unconformities in the Hermosa Formation near Coal Bank Pass, San Juan Mountains, Colorado. Mt. Geol. 39, 1–15.

Folk, R.L., Ward, W.C., 1957. Brazos River bar: a study in the significance of grain-size parameters. J. Sediment. Petrol. 27, 3–26.

Fouret, K.L., 1996. Deposition and diagenetic environments of the Mississippian Leadville Limestone at Lisbon Field, Utah. In: Huffman, A.C., Lund, W.R., Godwin, L.H. (Eds.), Geology and Resources of the Paradox Basin. Utah Geological Association, Salt Lake City, Utah, pp. 129–138.

Galarowski, T., 1976. New observations of the present-day suffusion (piping) processes in the Bereznica catchment basin in the Bieszczady Mountains (the East Carpathians). Stud. Geomorphol. Carpatho- Balc. 10, 115–122.

Goddard, E.N., Trask, P.D., DeFord, R.K., Rove, O.N., Singewald, J.T., Overbeck, R.M., 1948. Rock-Color Chart. Geological Society of America, Boulder. 16 pp.

Goossens, D., 1995. Field experiments in aeolian dust accumulation on rock fragment substrata. Sedimentology 42, 391–402.

Hall, J.F., 1990. The development of paleokarst and other solution features in the Mississippian Leadville Dolomite, central Colorado. In: Beaty, D.W., Landis, G.P., Thompson, T.B. (Eds.), Carbonate-Hosted Sulfide Deposits of the Central Colorado Mineral Belt. Society of Economic Geologists, Fort Collins, Monograph, vol. 7, pp. 108–117.

Harrel, J.A., Eriksson, K.A., 1979. Empirical conversion equations for thin-section and sieve derived size distribution parameters. J. Sediment. Petrol. 49, 273–280.

Horton, R.A., DeVoto, R.H., 1990. Dolomitization and diagenesis of the Leadville Limestone (Mississippian), central Colorado. In: Beaty, D.W., Landis, G.P., Thompson, T.B. (Eds.), Carbonate-Hosted Sulfide Deposits of the Central Colorado Mineral Belt. Society of Economic Geologists, Fort Collins, Monograph, vol. 7, pp. 86–107.

Iriondo, M., Krohling, D.M., 1997. The tropical loess. Proc 30th Intern. Geol. Congress, vol. 21, pp. 61–77.

Johnson, S.Y., 1989. Significance of loessite in the Maroon Formation (middle Pennsylvanian to lower Permian), Eagle Basin, northwest Colorado. J. Sediment. Petrol. 59, 782–791.

Jones, J.A.A., 1990. Piping effects in humid lands. In: Higgins, C.G., Coates, D.R. (Eds.), Groundwater Geomorphology: the Role of Subsurface Water in Earth-Surface Processes and Landforms. Geological Society of America, Special Paper, vol. 252, pp. 111–138.

Kessler, J.L.P., Soreghan, G.S., Wacker, H.J., 2001. Equatorial aridity in western Pangaea: lower Permian loessite and dolomitic paleosols in northeastern New Mexico, U.S.A. J. Sediment. Res. 71, 817–832.

Krinsley, D.H., Doornkamp, J.C., 1973. Atlas of Quartz Sand Grain Surface Textures. Cambridge University Press, New York. 91 pp.

Landis, G.P., Tschauder, R.J., 1990. Late Mississippian karst caves and Ba–Ag–Pb–Zn mineralization in central Colorado: Part II. Fluid inclusion, stable isotope, and rock geochemistry data and a model of ore deposition. In: Beaty, D.W., Landis, G.P., Thompson, T.B. (Eds.), Carbonate-Hosted Sulfide Deposits of the Central Colorado Mineral Belt. Society of Economic Geologists, Fort Collins, Monograph, vol. 7, pp. 339–366.

Larsen, E.S., Cross, W., 1956. Geology and petrology of the San Juan region, southwestern Colorado. USGS Prof. Paper, vol. 258. 303 pp.

Loope, D.B., Steiner, M.B., Rowe, C.M., Lancaster, N., 2004. Tropical westerlies over Pangaean sand seas. Sedimentology 51, 315–322.

Loucks, R.G., 1999. Paleocave carbonate reservoirs: origins, burial-depth modifications, spatial complexity, and reservoir implications. Am. Assoc. Pet. Geol. Bull. 83, 1795–1834.

Mack, G.H., James, W.C., Monger, H.C., 1993. Classification of paleosols. Geol. Soc. Amer. Bull. 105, 129–136.

Macleod, D.A., 1980. The origin of the red Mediterranean soils in Epirus, Greece. J. Soil Sci. 31, 125–136.

Maslyn, R.M., 1977. Fossil tower karst near Molas Lake, Colorado. Mt. Geol. 14, 17–25.

McKee, E.D., Gutschink, R.C., 1969. History of the Redwall Limestone of northern Arizona. Geol. Soc. Am., Mem. 114, 1–132.

Merrill, W.M., Winar, R.M., 1958. Molas and associated formations in the San Juan Basin–Needle Mountains area, southwestern Colorado. Am. Assoc. Pet. Geol. 42, 2107–2132.

Meyers, W.J., 1988. Paleokarstic features in Mississippian limestones, New Mexico. In: James, N.P., Choquette, P.W. (Eds.), Paleokarst. Springer-Verlag, New York, pp. 306–328.

Miller, K.B., McCahon, T.J., 2000. Eolian contribution to lower Permian (Wolfcampian) paleosols of the Kansas mid-continent. Geol. Soc. Am. Abstr. Programs 32 (7), A-255.

Moore, D.M., Reynolds, R.C., 1989. X-ray Diffraction and the Identification and Analysis of Clay Minerals. Oxford University Press, New York. 332 pp.

Muhs, D.R., Bush, C.A., Stewart, K.C., Rowland, T.R., Crittendon, R.C., 1990. Geochemical evidence of Saharan dust parent material for soils developed on Quaternary limestones of Caribbean and western Atlantic islands. Quat. Res. 33, 157–177.

Murray, H.F., 1958. Pennsylvanian stratigraphy of the Maroon Trough. Symposium on Pennsylvanian Rocks of Colorado and Adjacent Areas. Rocky Mountains Association of Geologists, Denver, pp. 47–58.

Musgrave, R.J., Webb, J.A., 2004. Paleomagnetic analysis of sediments in the Buchan Caves, southeastern Australia, provides a pre-late Pleistocene date for landscape and climate evolution. In: Saskowsky, I.D., Mylroie, J. (Eds.), Studies of Cave Sediments. Kluwer Academic/Plenum Publishers, New York, pp. 47–69.

Nettleton, W.D., Chadwick, O.A., 1996. Late Quaternary redeposited loess-soil development sequences, South Yemen. Geoderma 70, 21–36.

Palmer, A.N., Palmer, M.V., 1995. The Kaskaskia paleokarst of the northern Rocky Mountains and Black Hills, northwestern U.S.A. Carbonates Evaporites 10, 148–160.

Pelechaty, S.M., James, N.P., Kerans, C., Grotzinger, J.P., 1991. A middle Proterozoic paleokarst unconformity and associated sedimentary rocks, Elu Basin, northwest Canada. Sedimentation 38, 775–797.

Postek, M.T., Howard, K.S., Johnson, A.H., McMichael, K.A., 1980. Scanning-Electron Microscopy. Ladd Research Industries, New York. 305 pp.

Pye, K., 1987. Aeolian Dust and Dust Deposits. Academic Press, London. 334 pp.

Rapp, H., 1984. Are terra rossa soils in Europe eolian deposits from Africa? Geol. Foren. Stockh. Forh. 105, 161–168.

Reed, J.M., 2000. The Pennsylvanian Molas Formation of southwest Colorado: evaluation of the underlying paleokarst surface, previous terra rossa explanations, and diagenetic reddening. Unpubl. M.Sc. Thesis, Bowling Green State University, Bowling Green, Ohio, 121 pp.

Ross, C.A., Ross, J.R.P., 1985. Late Paleozoic depositional sequences are synchronous and worldwide. Geology 13, 194–197.

Sando, W.J., 1988. Madison Limestone (Mississippian) paleokarst: a geological synthesis. In: James, N.P., Choquette, P.W. (Eds.), Paleokarst. Springer-Verlag, New York, pp. 256–277.

Soreghan, G.S., 1992. Preservation and paleoclimatic significance of eolian dust in the Ancestral Rocky Mountains province. Geology 20, 1111–1114.

Soreghan, M.J., Soreghan, G.S., Hamilton, M.A., 2002. Paleowinds inferred from detrital zircon geochronology of upper Paleozoic loessite, western equatorial Pangaea. Geology 30 (8), 695–698.

Spoelhof, R.W., 1976. Pennsylvanian stratigraphy and paleotectonics of the western San Juan Mountains, southwestern Colorado. In: Epis, R.C., Weimer, R.J. (Eds.), Studies in Colorado Field Geology. Prof. Contrib. Colorado Sch. Mines, Golden, Colorado, vol. 8, pp. 159–179.

Syers, J.K., Jackson, M.L., Berkheiser, V.E., Clayton, R.N., Rex, R.W., 1969. Eolian influence on pedogenesis during the Quaternary. Soil Sci. 107, 421–427.

Symons, D.T.A., Lewchuk, M.T., Taylor, C.D., Harris, M.J., 2000. Age of the Sherman-type Zn–Pb–Ag deposits, Mosquito Range, Colorado. Econ. Geol. 95, 1498–1504.

Szabo, E., Wengerd, S.A., 1975. Stratigraphy and tectonogenesis of the Paradox Basin. In: Fassett, J.E. (Ed.), Canyonlands Country. Four Corners Geological Society, Durango, Colorado, 8th Field Conference, pp. 193–210.

Teller, R.W., Welder, F.A., 1983. Groundwater potential of the Leadville Limestone on the White River uplift in Garfield and Rio Blanco Counties, Colorado. USGS Water Res. Invest. Rep. 83-4036. 24 pp.

Tramp, K.L., Soreghan, G.S., Elmore, R., 2000. Integrated sedimentological, geochemical, and rock magnetic data as a high resolution record of pedogenesis in the Pennsylvanian Maroon Formation loessite (Colorado). Geol. Soc. Am. Abstr. Programs 32 (7), A255.

Tremul, A., 2002. Studio dei sedimenti della Grotta Pocala (Carso Triestino): analisi mineralogiche. Atti Mus. Civ. Stor. Nat. Trieste 49, 127–140.

Troutman, T.J., 2004. Reservoir characterization, paleogeomorphology, and genesis of the Mississippian Redwall Limestone paleokarst, Hualapai Indian reservation, Grand Canyon area, Arizona, U.S.A. Unpubl. M.Sc. Thesis, University of Texas, Austin, 221 pp.

Tschauder, R.J., Landis, G.P., Noyes, R.R., 1990. Late Mississippian karst caves and Ba–Ag–Pb–Zn mineralization in central Colorado: I. Geologic framework, mineralogy, and cave morphology. In: Beaty, D.W., Landis, G.P., Thompson, T.B. (Eds.), Carbonate-hosted Sulfide Deposits of the Central Colorado Mineral Belt. Society of Economic Geologists, Fort Collins, Monograph, vol. 7, pp. 308–338.

Tsoar, H., Pye, K., 1987. Dust transport and the question of desert loess formation. Sedimentation 34, 139–154.

Veevers, J.J., Powell, C.M., 1987. Late Paleozoic glacial episodes in Gondwanaland reflected in transgressive–regressive depositional sequences in Euramerica. Geol. Soc. Amer. Bull. 98, 475–487.

Villa, N., Dorn, R.I., Clark, J., 1995. Fine material in rock formations: aeolian dust or weathering? In: Tchakerian, V.P. (Ed.), Desert Aeolian Processes. Chapman and Hall, London, pp. 219–231.

Weimer, R.J., 1980. Recurrent movement on basement faults, a tectonic style for Colorado and adjacent areas. In: Kent, H.C., Porter, K.W. (Eds.), Colorado Geology. Rocky Mountain Association of Geologists, Denver, pp. 23–35.

Welton, J.E., 1984. SEM Petrology Atlas. American Association of Petroleum Geologists, Tulsa, Oklahoma. 237 pp.

Wengerd, S.A., Matheny, M.L., 1958. Pennsylvanian system of the Four Corners region. Am. Assoc. Pet. Geol. Bull. 42, 2048–2106.

Wengerd, S.A., Strickland, W.J., 1954. Pennsylvanian stratigraphy of Paradox Salt Basin, Four Corners region, Colorado and Utah. Am. Assoc. Pet. Geol. Bull. 38, 2157–2199.

White, W.B., 1990. Surface and near-surface karst landforms. In: Higgins, C.G., Coates, D.R. (Eds.), Groundwater Geomorphology: The Role of Subsurface Water in Earth-Surface Processes and Landforms. Geol. Soc. Am. Special Paper, vol. 252, pp. 157–175.

Wright, V.P., 1988. Paleokarsts and paleosols as indicators of paleoclimate and porosity evaluation: a case study from the Carboniferous of south Wales. In: James, N.P., Choquette, P.W. (Eds.), Paleokarst. Springer-Verlag, New York, pp. 329–341.

Yaalon, D.H., Ganor, E., 1973. The influence of dust on the soils of the Quaternary. Soil Sci. 116, 146–155.

Yaalon, D.H., Ganor, E., 1979. East Mediterranean trajectories of dust-carrying storms from the Sahara and Sinai. In: Morales, C. (Ed.), Saharan Dust. Wiley, Chichester, pp. 187–193.